Industrial Power Quality Enhancement using Fuzzy Logic Based Photovoltaic Integrated with Three Phase Shunt Hybrid Active Filter and Adaptive Controller

Soumya Ranjan Das
Department of Electrical Engineering, Parala Maharaja Engineering College Berhampur, India
srdas1984@gmail.com

Ambika Prasad Hota
Department of Electrical Engineering, Einstein Academy of Technology And Management Bhubaneswar, India
c117001@iiit-bh.ac.in

Hari Mohan Pandey
Department of Computer Science Engineering, Edge Hill University, United Kingdom
Pandeyh@edgehill.ac.uk

Biswa Mohan Sahoo
School of Computing & IT, Manipal University Jaipur, India
biswamohans@gmail.com

Abstract— Across the globe, solar photovoltaic (PV) sources are treated as the most favorable renewable sources which can fulfill a larger percentage of the total electricity demand with its clean form of energy. But due to its intermittent characteristics, the PV injects lots of uncertainty into the power system. Because of variation in input solar intensity due to climatic conditions, it will impact on the power quality (PQ) issues in power industries. Therefore, in this proposal, a solar PV integrated with shunt hybrid active filter (SHAF) is taken to fulfill the objective of (a) reducing the current harmonics and (b) supplying the active power generated from the PV system. The challenging task in the proposal is to control the PV variables and current control in voltage source inverter (VSI) of the SHAF. Therefore, three-key contributions are made as follows: (a) a control strategy designed which is based on adaptive notch filters (ANF) for reducing the harmonics by generating accurate reference currents; (b) a hysteresis controller is implemented for gating signal pulses; and (c) for maximum power tracking, a fuzzy based maximum power point tracking (MPPT) is developed for the solar tracker. We showed embedded applications of a SHAF for regulating the grid interfaced PV system. Besides, a SHAF operated with the ANF and based on the direct current control (DCC) method is used for computing the compensated current. A

comparative analysis has been done between ANF (least mean square (LMS) and recursive least square (RLS) method) and the existing non-adaptive notch filters (NNF). Rigorous computer simulations are performed to determine the effectiveness of the proposed system. The real-time digital simulator using OP 5142 designed with low cost and advanced monitoring capability is employed for validating results.

Keywords: - Harmonics, shunt hybrid filters, least mean square (LMS), power quality, recursive least square (RLS), total harmonic distortion (THD).

Abbreviations/Terms used

APF	: Active power filters
AFL	: Adaptive fuzzy logic control
ANF	: Adaptive notch filter
DCC	: Direct current control
FL	: Fuzzy logic control
LMS	: Least mean square
MPPT	: Maximum power point tracking
NNF	: Non-adaptive NF
P&O	: Perturb and observe
PQ	: Power quality
PV	: Photovoltaic
RLS	: Recursive least square
SHAF	: Shunt hybrid active filter
THD	: Total harmonic distortion
VSI	: Voltage source inverter
L_s, R_s	: Source inductance and resistance
C_{RF} , L_{RF}	: Ripple factor capacitance and inductance
C_D , V_D	: Capacitance and Voltage of DC Link
L_f	: AC inductor
K_P, K_I	: Proportional and integral gain
V_{MPP}, I_{MPP}	: Voltage and current at maximum power point

V_s, i_s : Supply voltage and current

i_f : Filter currents

i_L : Load current

P_{pv}, I_{pv}, V_{pv} : PV power, PV current, PV voltage

I_{ph} : Photo current

I_r : Reverse saturation current

I_{rr} : Diode reverse saturation current

$V_{oc\,pv}$: Open circuit PV voltage

r_s, r_p : Series, shunt resistances

q : Electron charge

k : Boltzmann constant

T : Ambient temperature

G : Power density of the solar insolation

T_r : Nominal temperature

I_{sc} : Short circuit current

α : Temperature coefficient

E_g : Band gap energy (1.1 ev)

N_s and M_s : Number of PV cells and number of the PV arrays connected in series

$i_{l\text{-}fu}$, $i_{l\text{-}h}$, $i_{l\text{-}q}$: Sinusoidal, harmonic and reactive current part of the load current

$X(n), W(n), \mu$: Input vector, coefficient vector and step size

1. Introduction

Nowadays renewable energy sources grip more attention in both research and real-time applications as these sources are plenty accessible on earth. In contrast to other renewable sources, solar energy is easy to harvest, convert and deliver to grid using different power converters [1]. Usually, dual scheme of PV systems are available in the grid interconnected system, i.e., grid linked and stand-alone systems. The grid linked is attached in shunt with the utility and supply solar energy to the grid whereas; stand-alone systems are attached with the load and electrical applications. The PV system is not capable to consider a constant DC source. The PV power output depends [2] on the type of load, temperature, and irradiation level. The maximum power point tracking (MPPT) is used for drawing the maximum power from the PV system. The PV system

should perform at MPPT to acquire maximum efficiency for different temperatures and levels of irradiations, which can be attained at a unique optimum point.

Different MPPT techniques are discussed in [3-5]. Among several controllers, the Perturb and Observe (P&O) [6] is the widely used MPPT technique because of its simple controlling design and easy operation. Further this technique also provides certain negative effects like slow tracking, less intelligence and less efficiency with sudden irradiance change. Moreover, the average power level is differed from the maximum power basically at less irradiance, sluggish time response, because of continuous oscillation around optimal point.

The cutting-edge technology in designing the MPPT uses the artificial intelligence such as fuzzy logic (FLC) [7], neural network [8] and neuro-fuzzy [9]. The benefits of utilising these methods are dynamic reaction and are more stable in comparison with the conventional methods. FLC is widely implemented because of its simple structure and easy to be developed. Some of the results show an improvement in efficiency or maximum power ratio using the FLC method.

Initially, the three factors i.e, inputs, error and change of error are required to be computed and during the computation the time response and accuracy of the MPPT gets exacerbate. But FLC provides certain demerits like not possible to find exact ample of the MPP. FLC is not suitable to operate with low irradiation and results high oscillations.

Therefore, in this literature an adaptive FL (AFL)-based MPPT [10-11] method is presented which is used to increase performance of the PV system. The proposed method offers several merits like its simple design with better precise results in comparison to other conventional methods. The performance of the MPPT approach provides improvement and a robust operation, rapid convergence speed, less oscillation and improved efficiency. The effectiveness and feasibility verifications of the proposed AFL-MPPT methodology are validated with considering various operating conditions at slow and fast change of solar radiation. The proposed AFL-MPPT method achieves accurate output power of the PV system with smooth and low ripple. In addition, the proposed AFL-MPPT method reaches steady state within very few seconds.

The implementation of PV energy is increasing day by day in the practical fields therefore large-scale PV generation is being introduced in the public domain. PV is treated as the most favorable renewable sources which can fulfill a larger percentage of the total electricity demand. It is clean form of energy but inject lots of uncertainty into the power system because of its intermittent characteristics. Because of variation in input solar intensity due to climatic conditions, it will

impact on the power quality (PQ), protection and stability issues in power industries. Again, being inverter based distributed generation (DG), integration of these resources will affect the protection methodology utilized in conventional power system.

In this proposed framework, it's a highly challenging task to deal with the PQ issues occurring in power system with large penetration of solar PV and other renewable resources. Different PQ disturbances may occur in the power which may threat the reliability of the electricity supply**.**

Hence, shunt hybrid active filter (SHAF) is employed for minimizing the PQ disturbances. In this paper, a grid interfaced solar PV with SHAF is proposed which performs dual role; supply maximum power tracked from the PV array to the grid and improve the PQ in the distribution system by reducing the harmonics in the supply current, balancing the supply currents and managing the reactive power. Usually, it is often seen that PQ issues like large harmonics and flicker, influence large scale PV integrated generation system. The grid integrated PV generates complicated PQ issues and therefore affects the sinusoidal voltage and current waveform which thereby reduces the efficiency of the system, raises the heating of transformer, growth in malfunction of motors and cables and life span of PV modules is inadequate. In recent years, grid pollution has become more and more severe, mainly due to increase of non-linear loads. Therefore, the electronics equipment utilized in the power system must obey the basic harmonics standard, such as IEEE-519 to provide high PQ. In this aspect, a SHAF is implemented in this literature whose purpose is to feed extracted power from PV to the supply system and also compensation in harmonics and reactive power. Moreover, to comprise the PQ improvement features the detection of harmonic and reactive currents is compulsory.

Therefore, to improve the quality of power in three-phase power distribution system, an effective control technique is required which can perform better in synchronising the PV integrated shunt hybrid filter under balanced and unbalanced non-linear load.

Different frequency and time domain control approaches are discussed in [12-14] for controlling the Voltage Source Inverter (VSI) of the SHAF. The synchronously reference frame (SRF) or d-q theory and instantaneous p-q theory are performed widely to produce reference signals for compensating the harmonic currents. Moreover, some other techniques like artificial neural networks (ANN) and Fast Fourier transforms (FFT) are discussed in [15-16]. In [17], the author discussed several ANN techniques for generating the reference currents and active power filtering. However, the performance of the above techniques is strongly affected by supply distorted voltage

and frequency variations.

The notch filter (NF) [18] which is further introduced is found to be an effective approach for improving filtering capability, stability, and selective cancellation of harmonic components. The NFs can be divided into two major categories: non-adaptive NF (NNF) [19] and adaptive notch filter ANF [20-21]. The NNF offer a fast dynamic response and a high harmonic filtering capability. They, however, cannot sufficiently mitigate the grid voltage unbalance [22]. When the grid frequency fluctuates, the harmonic rejection capability of an NNF is weakened.

The ANF is one of the advanced algorithms, introduced as an effective control method for extracting the reference sinusoidal components from the disturbed input signal because it can follow the frequency variations of the input signal by changing the Notch frequency. The notch frequency of an ANF can be adjusted to maintain strong filtering capability under this circumstance. The ANF is a common adaptive design that is used to extract the preferred sinusoidal component for a given signal by tracking the frequency variations. ANF draws positive-sequence components from non-ideal voltages and provides dynamic reaction in comparison to other standard signal processing units. The ANF is highly insensitive to PQ disturbances in the grid network.

In this paper, a comparison work has been analyzed using both NNF and ANF methods under different loading conditions in the distribution system. Further in ANF two different techniques i.e, least mean square (LMS) and recursive least square (RLS) are employed for further investigations based on direct current control (DCC) to accomplish the extraction of harmonics in the distribution system. The LMS technique [23] is designed based on linear adaptive filtering with the objectives that the output is computed by the adaptive filter based on the estimation of the errors between the outputs and the desired response and the weights are updated automatically for minimizing the error. RLS algorithm is a self-adaptive algorithm [24] and is extensively implemented in many applications due to its simple structure and robust performance. RLS technique is effective in reducing the noise and automatically adjusts the parameters under different operating conditions. Both the techniques are suitable in ANF to estimate the harmonic currents.

The main purpose of the proposed method is to offers dual benefits of supplying solar energy into the grid and also to the load (during breakdown of the grid) by a dc/dc boost converter and

reducing the harmonics that affects the PQ in the utility system by controlling the VSI of the SHAF, balancing the grid currents and managing the reactive power.

In this paper, a three-phase SHAF integrated with PV system is implemented to improve the PQ. The proposed methodology offers dual benefits of supplying solar energy into the power system by a dc/dc boost converter and reducing the harmonics that affects the PQ in the utility system by controlling the VSI of the SHAF. The control of grid integrated with solar PV is carried out using MPPT.

The main contributions of this paper are highlighted as follows:

a) Firstly, we propose a fuzzy-based PV integrated with a three-phase SHAF that uses adaptive controllers. Here, we aim to achieve two objectives: to supply the active power generated from the PV system and to reduce the current harmonics by supplying the compensation current at the point of common coupling.
b) Secondly, a MPPT technique uses an adaptive fuzzy logic is implemented for tracking the maximum power from the solar PV and to achieve more efficiency.
c) Thirdly, an ANF based on the DCC is conducted to accomplish the extraction and reduction of harmonics in the distribution systems. The performance of the ANF is compared with the existing NNF technique.
d) Fourthly, extensive computer simulations are made to calculate the effectiveness of the proposed system. Performance is analyzed using ANF with LMS and RLS methods. On other hand, for generating the gating signals the hysteresis controller is used.
e) Finally, the performance of the proposed technique is demonstrated by producing extensive simulation outcomes which shows the harmonics compensation obeys the IEEE-519 standard and the performance of the proposed technique is validated with experimental results.

The remaining paper is structured as follows. The configuration of SHAF is discussed in Section 2. The control strategy for PV and VSI of SHAF is provided in Section 3. The analysis of simulation output is provided in Section 4. The conclusion is discussed in Section 5.

2. System Design

A single line diagram of PV integrated SHAF in three-phase network is depicted in Fig. 1, and the detailed configuration is presented in Fig. 2. The proposed model represents a three-phase grid system, with PV coupled to the DC bus system. The DC/DC boost converter is incorporated to the capacitor of the VSI which is regulated by using appropriate MPPT.

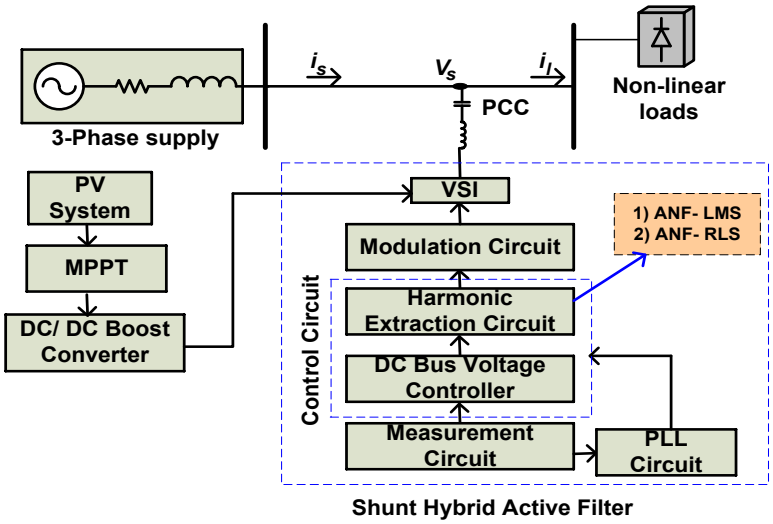

Fig. 1. Single line diagram of PV integrated SHAF in three-phase supply system.

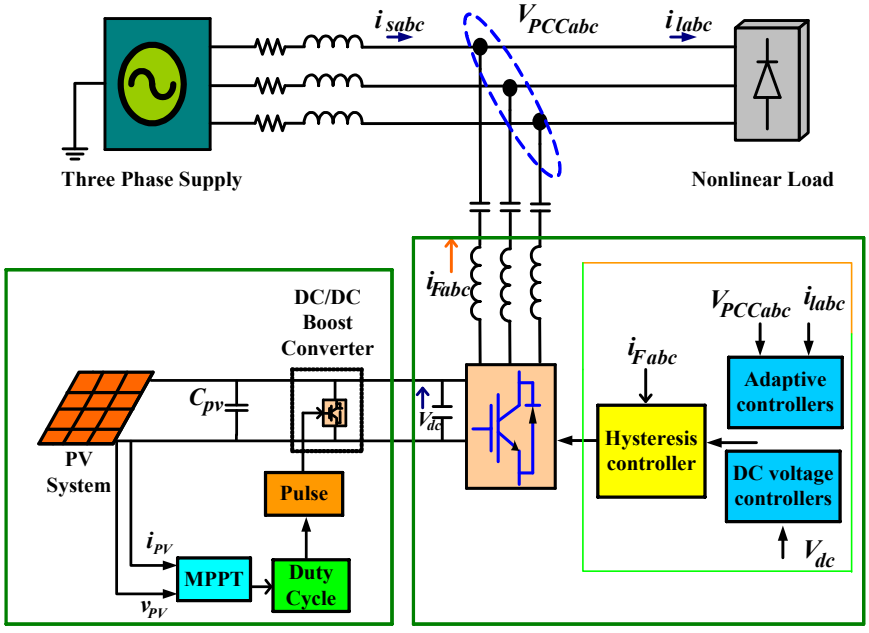

Fig. 2. Detailed configuration of PV integrated SHAF in three phase supply system .

The boost converter produces an output voltage which is connected to the DC bus of the inverter. The DC bus is linked to VSI with a capacitor. The MPPT approach is performed drawing maximum possible energy from solar energies. Therefore, the maximum energy drawn is provided to the grid through the SHAF. For controlling the PV system, variable step size P&O MPPT is developed for maximum power tracking. The gating signal is made using hysteresis controller. The reference current computation is computed by engaging DCC approach with ANF. The PV

equivalent circuit [25] is presented in Fig. 3. The PV cell output current I_{pv}, photo current I_{ph}, reverse saturation current I_r, diode reverse saturation current I_{rr}, PV array voltage V_{pv}, and open circuit PV voltage $V_{oc\,pv}$ are expressed in Eq. (1) – (6).

$$I_{PV} = I_{Ph} - I_r\left[e^{q(V+I_{PV}r_s)/\mu KT} - 1\right] - \frac{V + I_{PV}r_s}{r_P} \tag{1}$$

$$I_{Ph} = \left[I_{sc} + \alpha\left(T - T_r\right)\right]\frac{G}{1000} \tag{2}$$

$$I_r = I_{rr}\left(\frac{T}{T_r}\right)^3 e^{\left[\left(qE_g/\mu K\right)\left((1/T_r)-(1/T)\right)\right]} \tag{3}$$

$$I_{rr} = \frac{I_{sc} - \left(V_{oc}/r_P\right)}{e^{qV_{oc}/\mu KT_r} - 1} \tag{4}$$

$$V_{PV} = VN_sM_s \tag{5}$$

$$V_{oc-pv} = V_{oc}N_sM_s \tag{6}$$

Where, r_s, r_p q η k T G T_r I_{sc} α E_g N_s and M_s are the series, shunt resistances, electron charge, ideality factor of the junction *p-n*; Boltzmann constant, ambient temperature; power density of the solar insolation, nominal temperature, short circuit current, temperature coefficient, band gap energy (1.1 eV), number of PV cells and number of the PV arrays connected in series respectively.

3. Control Strategy

3.1 Controlling of PV using MPPT Technique

3.1.1 Adaptive Fuzzy Logic Control

In solar PV system, the non-linearity of solar panels and environmental effect makes the tracking performance more complexity which can be solved by using FL based MPPT which requires less data and simple design, does not need any mathematical modelling, fast time response solve the systems non-linearity and are more stable. Application of FL techniques to track the maximum power point in PV systems has become more accessible because of the improved performance and low cost of micro controllers. FL achieves vastly improved performance for MPPT technique in terms of speed response and low fluctuation about the maximum power point.

The FL based MPPT operates in three different stages which comprises of fuzzification, fuzzy inference mechanisms (rule base table lookup) or evaluation, and defuzzification. In fuzzification stage, numerical input variables are transformed to linguistic variables based on the membership

functions used; the more the membership functions used the better the performance of the FL controller. Defuzzification provides the controller output where the linguistic variables are transformed into numeric variables supplying the analog signals for controlling the duty cycle of the power converter and therefore to obtain the MPP. In addition, it has a rule table in which the designed rules are stored. The FLC performs the calculation process which is called as rule inference. The generated inference system consists of two inputs (open circuit voltage and short circuit current) and one output (the desired duty cycle). The FL can effectively deal with the nonlinearity in the I–V characteristics of PV systems.

The output signifies to the duty cycle command (ΔD) for the boost converter. The output of FL is compared with sawtooth triangular signal and the comparator produces the duty cycle for the power converter in accordance. In the proposed controller, the inputs are considered to be error (E) and the change of error (ΔE) values. The values of error signal is calculated as the ratio of variation in the PV extracted output power to the variation in the PV output voltage and are expressed as Eq. (7) – (8).

$$E(n) = \frac{P(i) - P(i-1)}{V(i) - V(i-1)} \tag{7}$$

$$\Delta E(i) = E(i) - E(i-1) \tag{8}$$

The term $P(i)$, $V(i)$ and $E(i)$ denote the present samples of the PV output power, voltage and error variable respectively. While $P(i-1)$, $V(i-1)$ and $E(i-1)$ denotes the previous sample of the PV output power, voltage, and error variable respectively. The values of E and ΔE are computed by measuring the output power and voltage of the PV panel based on (7) and (8). In the proposed MPPT the input MFs are considered to be E and ΔE with 7X7 fuzzy rule using different MFs like normal (N), heavy (H), more heavy (MH) and extra more heavy (EMH), light (L), more light (ML) and extra very weak (EML). As soon as the proposed MPPT measures the values of E and ΔE, the FL converts the existing variables into linguistic values.

Table 1: 7X7 Fuzzy rule base for AFL MPPT technique.

ΔE / E	EML	ML	L	N	H	MH	EMH
EML	EML	EML	EML	EML	ML	L	N
ML	EML	EML	EML	ML	L	N	H
W	EML	EML	ML	L	N	H	MH
N	EML	ML	L	N	H	MH	EMH
S	ML	L	N	H	MH	EMH	EMH
VS	W	N	S	VS	POB	EVS	EVS
EVS	N	S	VS	EVS	EVS	EVS	EVS

The fuzzy rule base is presented in Table 1 and the controlling structure is illustrated in Fig. 3. The fuzzy rule is made based on the type of MF used. The triangular MFs are usually applied because it is simple and easy in application with minimal computational efforts. The Fuzzy rules with less numbers are never considered because it is not capable to maintain the DC link voltage at the desired level.

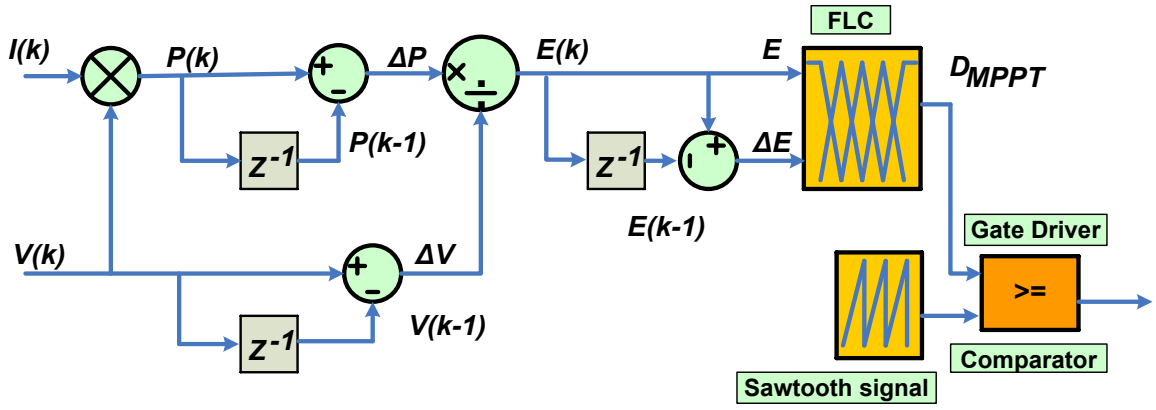

Fig. 3. Controlling structure of the AFL-MPPT method with two inputs and one output.

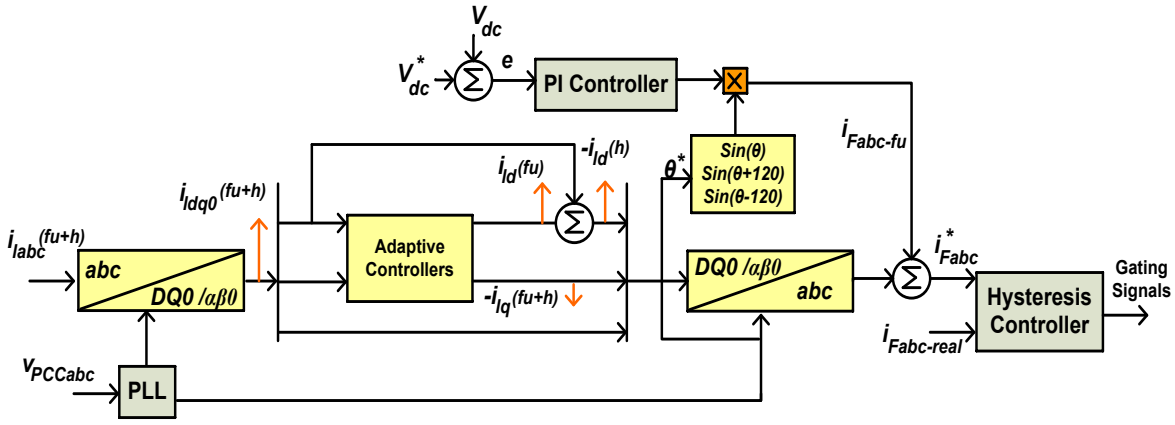

Fig. 4. Block diagram of the adaptive filter for controlling the VSI for harmonic current extraction and switching signal.

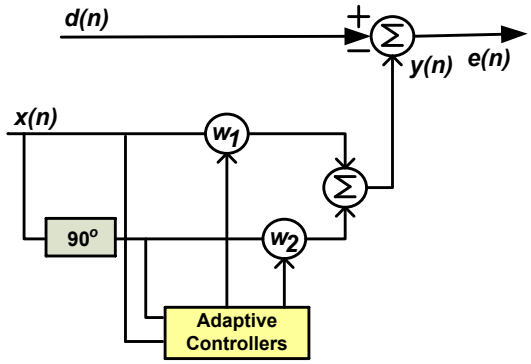

Fig. 5. Block diagram of ANF

3.2 Controlling of VSI using compensating signals generation Techniques

The control strategy of controlling the VSI for harmonic current extraction and switching signal is illustrated in Fig. 4 and the block diagram of ANF is illustrated in Fig. 5. Here, the DCC approach is used for regulating the VSI of SHAF in terms of reference current calculation. The supply current is forced to be harmonic free and simultaneously in phase with voltage at PCC.

Therefore, the overall grid current is given using Eq. (9).

$$i_s(t) = i_l(t) + i_F(t) \tag{9}$$

The load current comprises three current components as shown in Eq. (10).

$$i_l(t) = i_{l-Fu}(t) + i_{l-h}(t) + i_{l-q}(t) \tag{10}$$

Where, Fu, h and q represent the sinusoidal part, harmonic part, and reactive current part of the load current.

Here, two different ANF techniques i.e, ANF-LMS and ANF-RLS are employed for eliminating the load harmonics. These techniques usually compute the real part of the load current and deducted from the sensed current.

3.2.1 ANF-LMS

Let, $d(n)$, signifies the non-linear load current and $x(n)$, signifies the fundamental component. The reference input $x(n)$ is managed by the ANF generating the output signal $y(n)$ that tracks the difference in the fundamental component of the load current.

The recursion procedure of the LMS approach is expressed in Eq. (11) - (14).

$$e(n) = d(n) - y(n) = d(n) - X^T(n)W(n) \tag{11}$$

$$W(n+1) = W(n) + \mu e(n) X(n) \tag{12}$$

$X(n), W(n), \mu$ signifies input vector, coefficient vector and step size.

$$w_1(n+1) = w_1(n) + \mu e(n) x(n) \tag{13}$$

$$w_2(n+1) = w_2(n) + \mu e(n) x_{90}(n) \tag{14}$$

$x_{90}(n) = x(n)$, Phase shift of 90^0.

3.2.2 ANF-RLS

The recursion process of the RLS algorithm is given under several steps:

First step- Initialization, $M_{\lambda 1}(0) = 0.1, M_{\lambda 2}(0) = 0.1,\ w_1(0) = 0, w_2(0) = 0, \lambda = 0.9$

Second step-Computing gain

$$G_1(n) = \frac{M_{\lambda 1}(n-1) x(n)}{\lambda + x^2(n) M_{\lambda 2}(n-1)} \tag{15}$$

$$G_2(n) = \frac{M_{\lambda 2}(n-1) x_{90}(n)}{\lambda + x^2{}_{90}(n) M_{\lambda 2}(n-1)} \tag{16}$$

Third step-Computing output and error

$$y(n) = w_1(n-1) x(n) + w_2(n-1) x_{90}(n) \tag{17}$$

$$e(n) = d(n) - y(n) \tag{18}$$

Fourth step- Coefficient adaptation

$$w_1(n) = w_1(n-1) + G_1(n) e(n) \tag{19}$$

$$w_2(n) = w_1(n-1) + G_2(n)e(n) \tag{20}$$

Fifth step- Inverted autocorrelation coefficients

$$M_{\lambda 1}(n) = \lambda^{-1} M_{\lambda 1}(n-1) - \lambda^{-1} G_{\lambda 1}(n) x(n) M_{\lambda 1}(n-1) \tag{21}$$

$$M_{\lambda 2}(n) = \lambda^{-1} M_{\lambda 2}(n-1) - \lambda^{-1} G_{\lambda 2}(n) x_{90}(n) M_{\lambda 2}(n-1) \tag{22}$$

Where, λ is considered as forgetting factor which is nearly equal to one but less than it.

4. Simulation Model

In this paper, a three-phase, grid linked PV with single-stage, energy conversion system is developed with MATLAB/ Simulink tool. The PV system projected in this literature performs two basic functions. First, it injects extracted solar power in the grid and second, it helps in PQ improvement in three-phase system. To validate the feature of PQ, two types of loads (linear and non-linear) are taken under consideration. Initially, using a linear load, reactive power control and source currents balancing characteristics are presented while, with non-linear load, the harmonics elimination and grid currents balancing features are presented along with real power inclusion into the grid and power rating of 10 kW for both types of loads. A PV with 25 kW rating is taken for consideration. The system parameters are provided in Table 2.

Table 2. Parameter used in Simulation

Parameters	Value
3-Phase Line voltage, Frequency	400V,50Hz
Line impedance	L_s= 2Mh/ phase, R_S=0.010Ω
Ripple Filter	C_{RF} = 50 µF , L_{RF} =0.68mH
Active Filter parameters	C_D = 3000µF V_D=750V
AC inductor	L_f= 3.3mH
Controller gain	K_P=24, K_I=1.2
Hysteresis Band Limit	0.5A
Sampling time	$2e^{-4}$ seconds
short circuit current	I_{scn} = 8.2 A,
open circuit voltage	V_{ocn} = 35V
Short circuit current	I_{sc} =10A
panel voltage at MPP	V_{MPP} =28V
panel current at MPP	I_{MPP} = 7.5A
number of series panels	25
number of parallel panels	3
Switching frequency	5 KHz

The significant signals features of the system are provided in results. The variables V_s, i_s, i_L, i_{VSC}, P_{pv}, I_{pv}, V_{pv} are considered as three-phase line voltages, supply, load and filter currents, PV power, PV current, PV voltage, respectively.

4.1 System behavior under balanced non-linear Load

At this mode of operation, the performance of the system is provided in Fig. 6-9. The proposed system uses a non-linear load of 100 kW at 0.8 lagging power factor and system performance is shown for 0 to 0.25s. Initially, the system is working at power factor correction mode. From *Ppv* (see Fig. 6, 8), it can be noticed that the PV power is maintained at100 kW. If the PV power is more than 100 kW, then the difference power will be supplied to the grid. During the period from 0 sec to 0.1 sec, one of the load phase 'c' is opened. During the period, removal of load current leads to unbalance in the load and moreover the VSI currents are completely unbalanced to maintain the source currents balanced. At 0.1 sec, the dynamic response of the system is noticed during addition of the load.

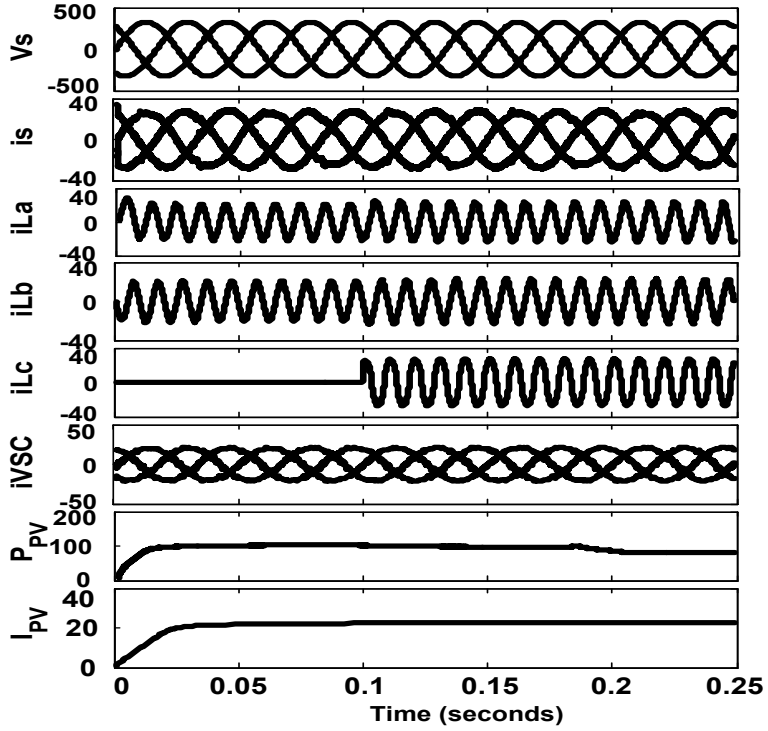

Fig. 6. System behavior showing source, load, and filter current with PV power and current, under balanced non-linear load using ANF-LMS.

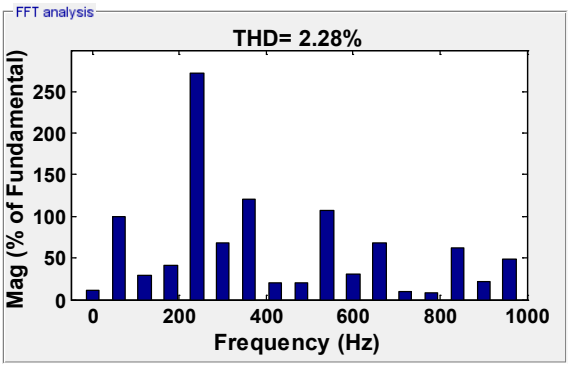

Fig. 7. THD value of source current

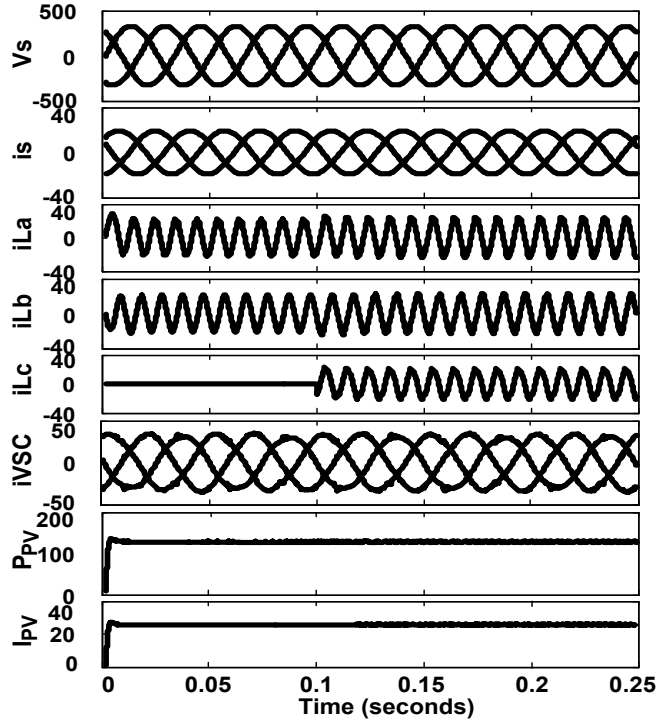

Fig. 8. System behavior showing source, load and filter current with PV power and current, under balanced non-linear load using ANF-RLS.

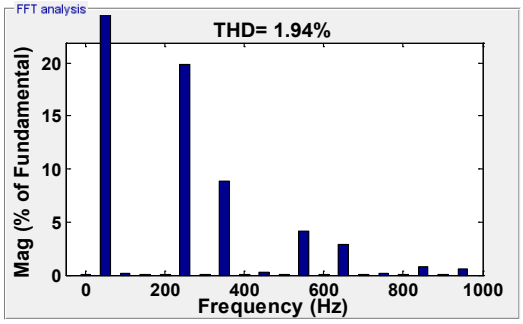

Fig. 9. THD value of source current.

Fig. 6 illustrates the simulation outcomes of variable parameters of the proposed system showing three phase source, load and filter current, PV current and power. The total harmonic distortion (THD) analysis of source current is presented in Fig. 7. The percentage THD value found to be 2.28%. The above cases are carried out under ANF-LMS technique. Similarly, same mode of operation is carried out under ANF-RLS technique. The corresponding simulation results are produced in Fig. 8. While the percentage THD analysis is found to be 1.94% and is shown in Fig. 9, which shows an improved result compared to the previous controller.

Further, the simulation work is also done under balanced non-linear condition using NNF technique. The results of different parameters like the supply voltage, source current, individual three-phase load currents, compensating current, PV power and PV current is noticed in Fig. 10 with the time period of 0 to 0.25 seconds. The behavior of the source currents in comparison to the ANF technique gets reduced due to weak harmonic rejection capability of NNF. The THD of the source current is illustrated in Fig. 11 and found to be 3.12% which is high in comparison to the proposed ANF techniques.

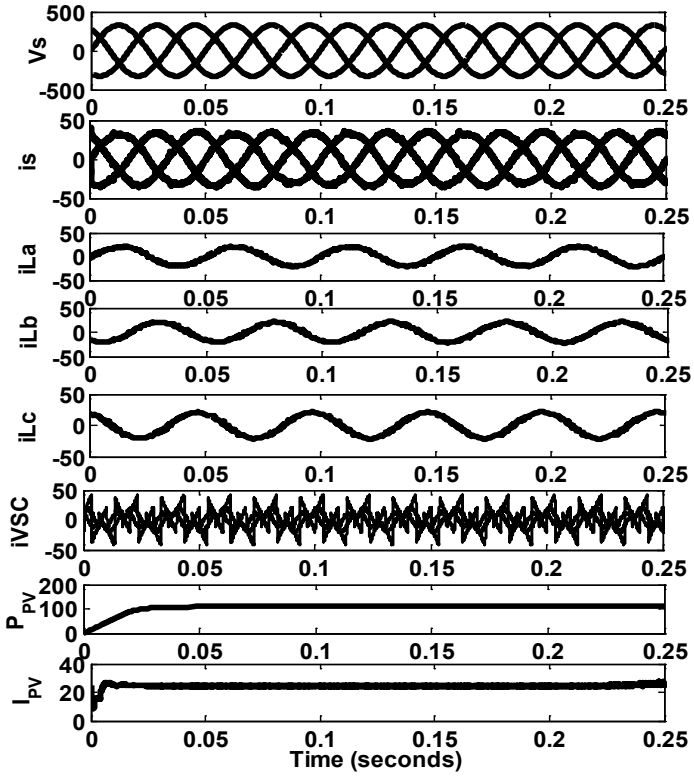

Fig. 10. System behavior showing source, load and filter current with PV power and current, under balanced non-linear load using NNF technique.

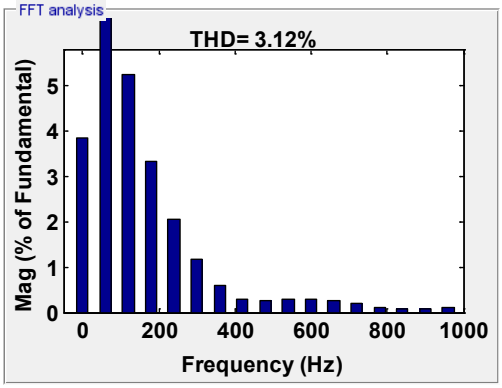

Fig. 11. THD value of source current.

4.2 System behavior under unbalanced non-linear load

This subsection discusses the performance of the system under non-linear unbalanced load which is illustrated in Fig. 12-15. The proposed system uses a non-linear load of 100 kW. The performance of the system is shown for 0 to 0.25s. During, t = 0.1 s, one of the load phase 'c' is removed, the system performance is analysed in Fig.10 for phase 'c'. The removal of load current leads to unbalance in the load and moreover the VSI currents are completely unbalanced to maintain the balanced source currents.

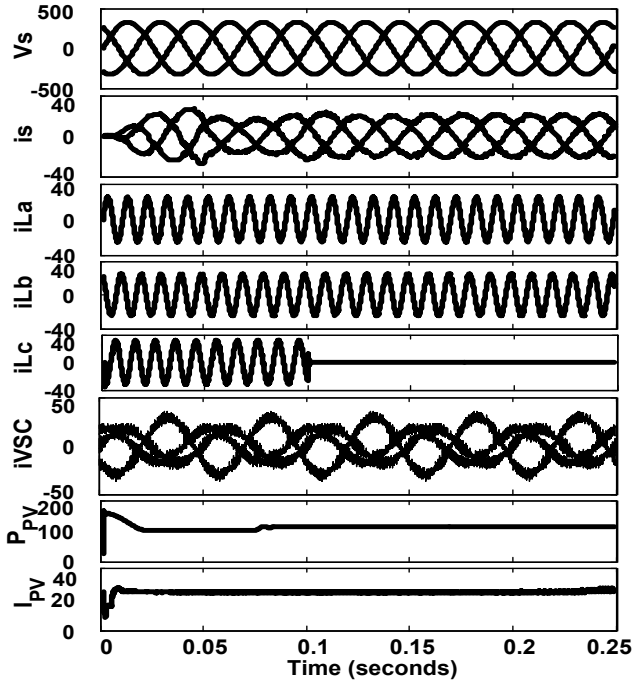

Fig. 12. System behavior showing source, load, and filter current with PV power and current, under unbalanced non-linear load using ANF-LMS.

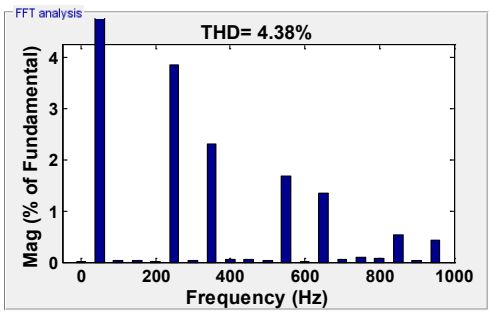

Fig. 13. THD value of source current.

The simulation results show under transient response of the load current with distortions in supply currents. The corresponding PV power and current are illustrated in Fig. 12 and the percentage THD is observed at 4.38%. The THD analysis is shown in Fig. 13. The above cases are carried out under ANF-LMS technique. Similar mode of operation is carried out under ANF-RLS technique. The corresponding simulation results are produced in Fig. 14. While the percentage THD analysis is found to be 3.96% and is shown in Fig. 15, which shows an improved result compared to the previous controller.

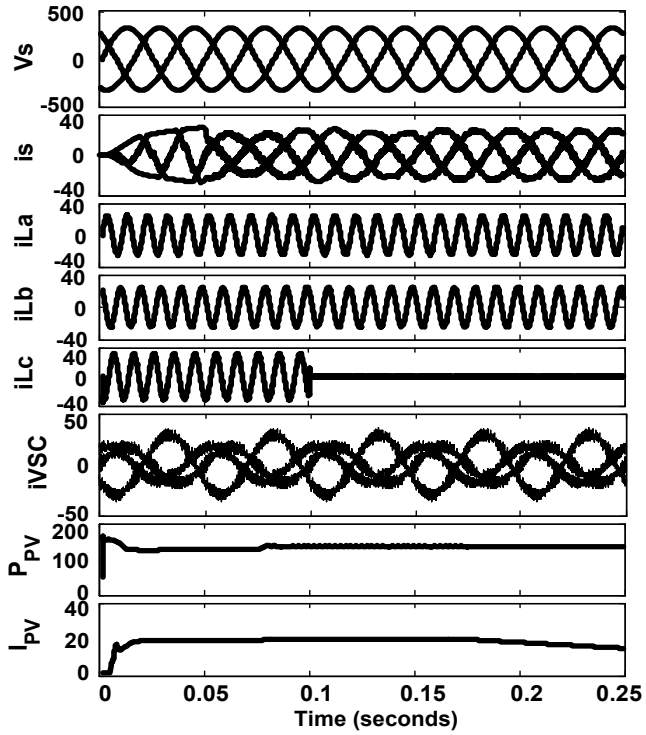

Fig. 14. System behavior showing source, load, and filter current with PV power and current, under unbalanced non-linear load using ANF-RLS.

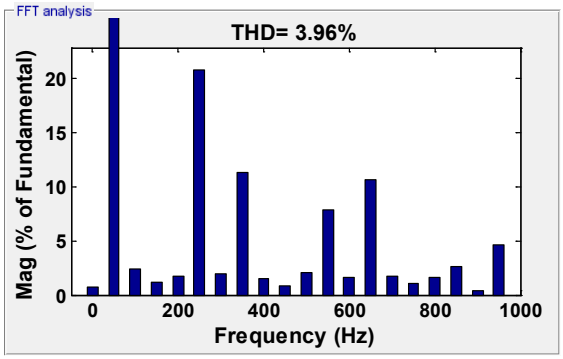

Fig. 15. THD value of source current.

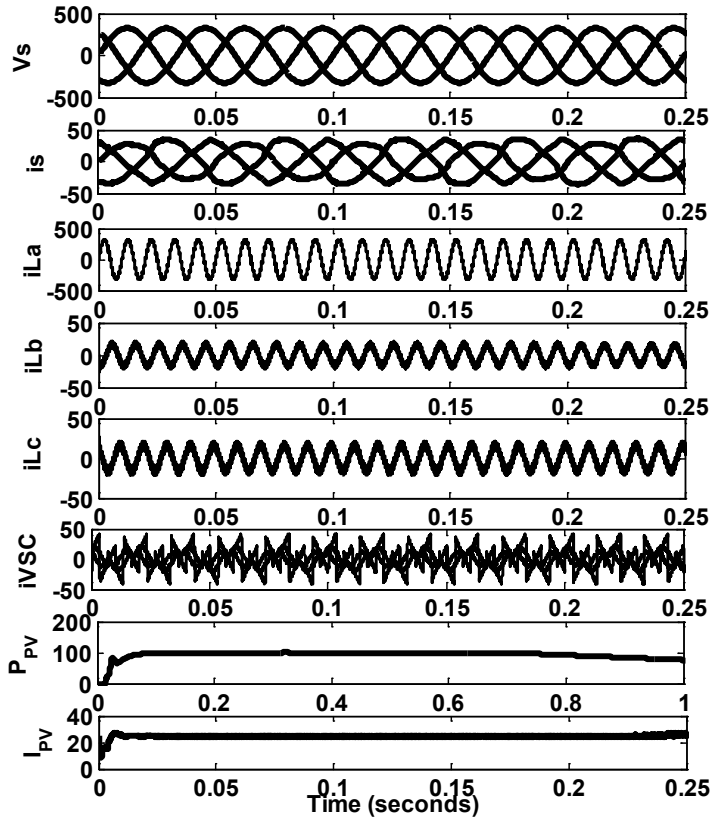

Fig. 16. System behavior showing source, load and filter current with PV power and current, under unbalanced non-linear load using NNF.

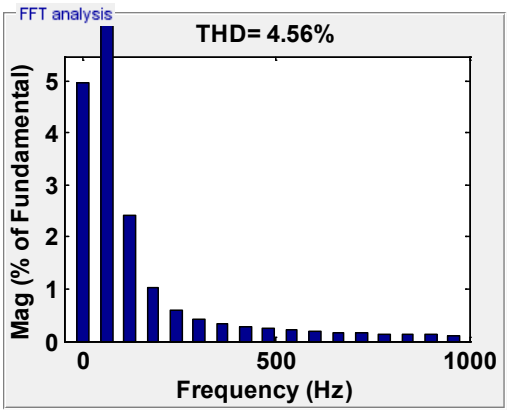

Fig. 17. THD value of source current.

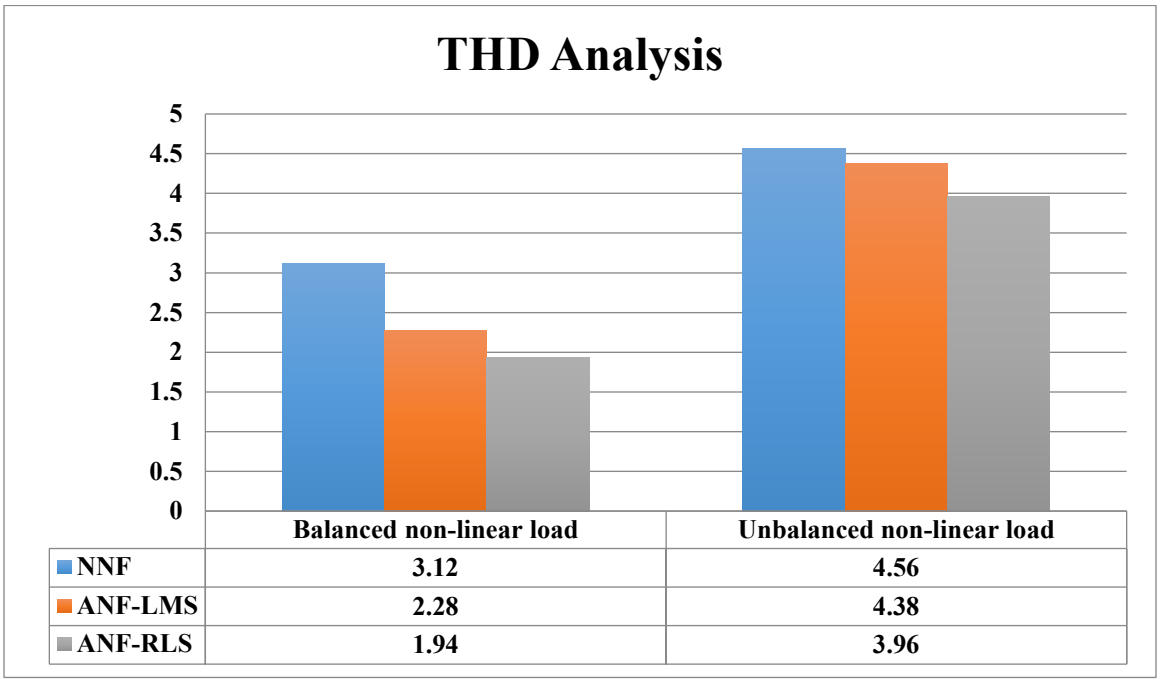

Fig. 18. Comparative THD analysis of source current using NNF, ANF-LMS and ANF-RLS techniques.

4.3 Dynamic Response

The dynamic reaction for low variation in solar insolation is illustrated in Fig. 19 and Fig. 20. The reaction for fast ramp decline in solar insolation (500 W/m^2 /s) is expressed in Fig. 19. The irradiance is varied from 1000 to 500 W/m^2. As load current is maintained constant, therefore, the load power is also maintained. As the insolation drops, the power provided to the grid and grid

current decreases. Due to drop of solar irradiance, I_{pv} is reduced in subsequent steady state form. Fig. 20 provides the reaction of system for fast ramp increase in insolation (500 W/m^2 /s). The maximum PV power gets increased with increase in insolation.

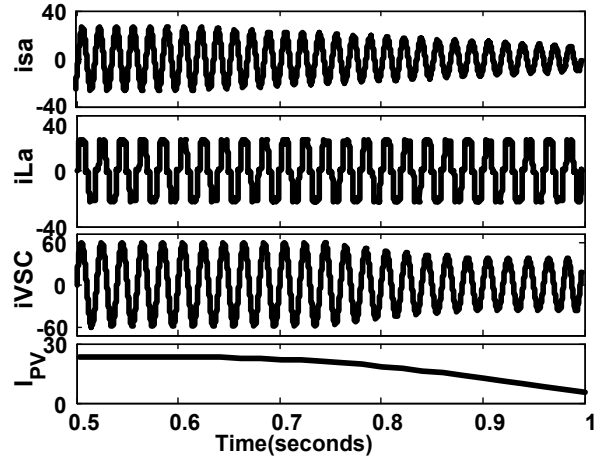

Fig. 19. Dynamic response of the system for decrease in solar insolation.

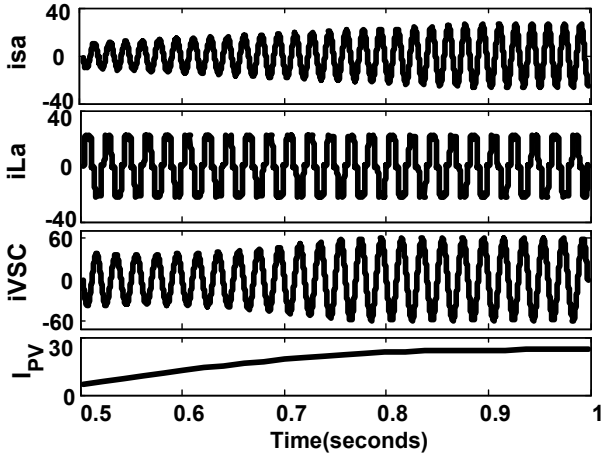

Fig. 20. Dynamic response of the system for increase in solar insolation.

4.4 Opal-RT Results and Analysis

The real-time validation of the stability study in PV integrated power system is illustrated in this sub-section. The considered power system as displayed in Fig. 1 has been developed in MATLAB 2013a. The simulated model is then formulated in OPAL-RT and dumped in for the real-time simulation. The real-time digital simulator using OP 5142 is designed with low cost, highly commercial off the shelf (COTS) components having advanced monitoring capability. It consists of a powerful target PC with 3.3 GHz processor with the operating system of Red Hat Linux,

FPGA-based I/O management, Xilinx Spartan 3, Virtex FPGA processor. It has 8 signal conditioning ADC module with 16/32 channels, 128 analog/256 discrete/mixture of analog and digital signals. It can network with more than 3000 I/O channels at a tie step of 25 microseconds having a provision of hardware-in-loop testing. Fig. 21 (a) shows the real-time experimental set-up using OPAL-RT OP 5142. The source voltage along with the source current during balance load using ANF-LMS and ANF-RLS is depicted in Fig. 21 (b) and 21 (c). The performance of the filter with the source voltage along with the source current during unbalance load using ANF-LMS and ANF-RLS is depicted in Fig. 21 (d) and 21 (e). The distortions in supply current are due to the existence of non-linear load which could be eliminated by injecting filter current at PCC. The parameters of the system for real-time experiments are the same as that of the simulation parameters. of the system are being incorporated with the hybrid power system.

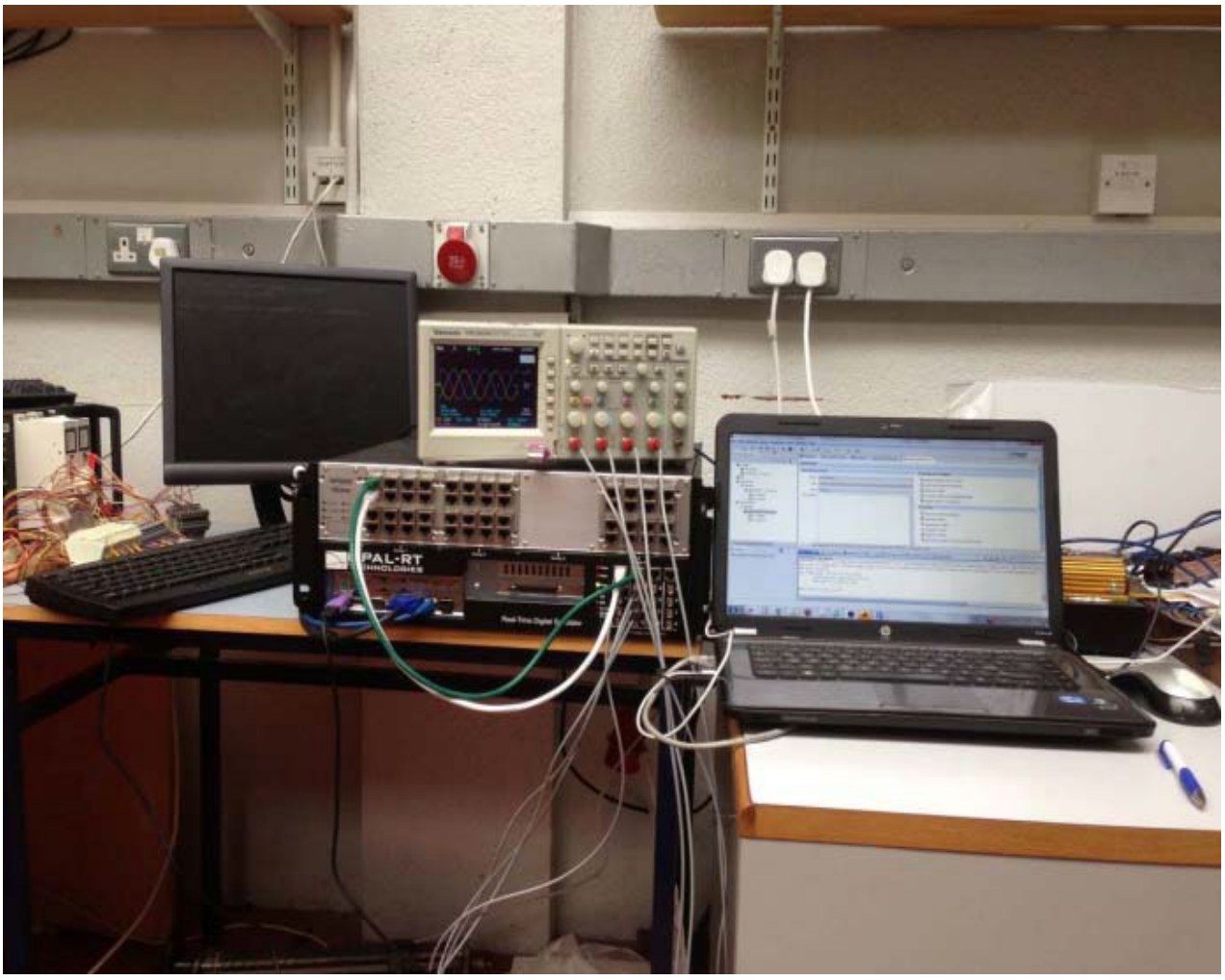

(a)

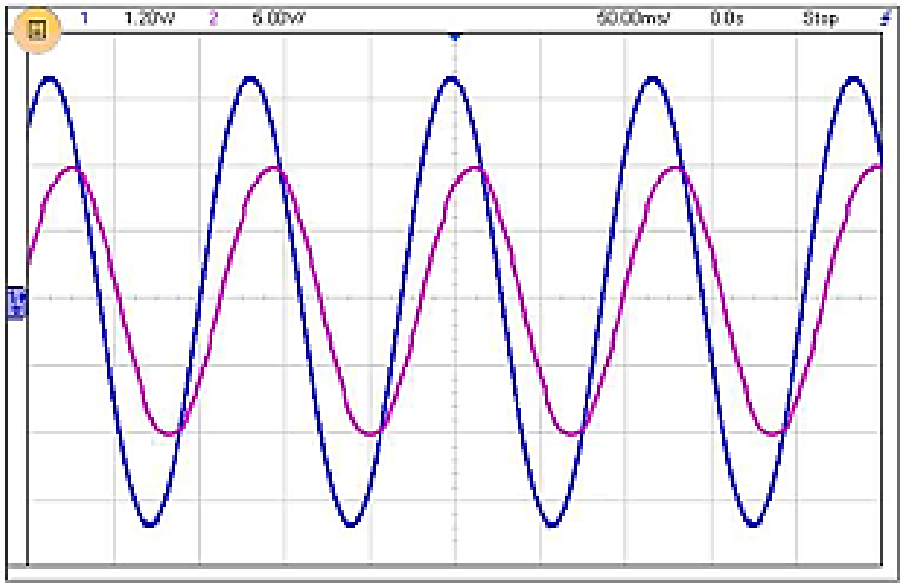

(b)

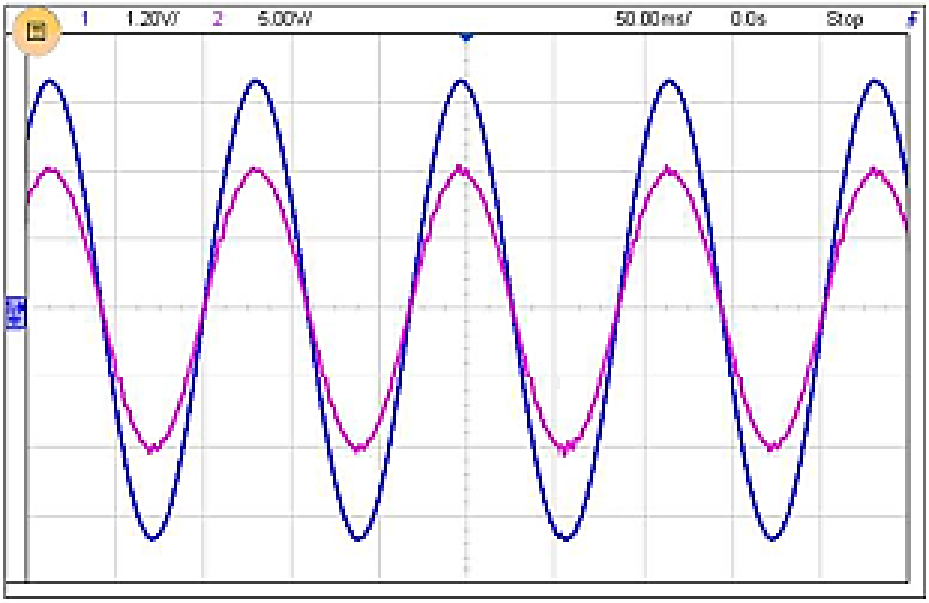

(c)

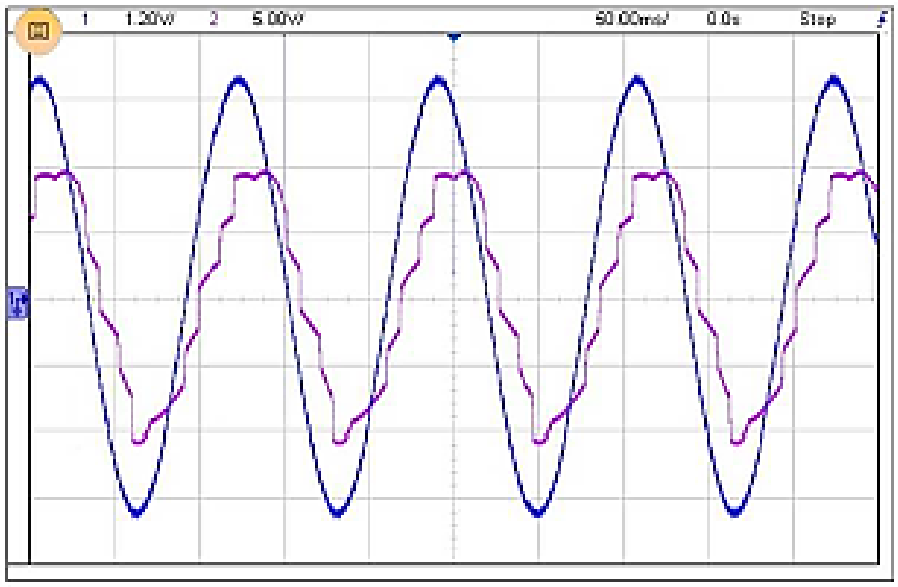

(d)

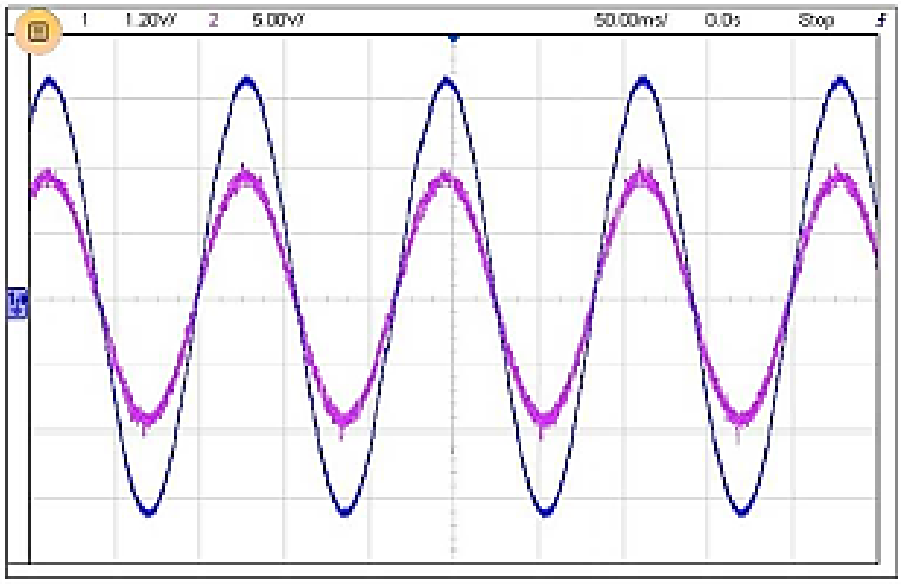

(e)

Fig. 21. (a) OPAL-RT setup; Source voltage (high magnitude) and source current (low magnitude), during balance load using (b) ANF-LMS and (c) ANF-RLS; and during unbalance load using (c) ANF-LMS (d) ANF-RLS.

5. Conclusions

In this paper, we have presented a modified MPPT technique suitable to track the maximum power from the PV system. The efficiency of the proposed system has been found superior as compared to the conventional P&O technique. With the steady-state situation, the proposed system

has provided rapid convergence speed and less oscillation. Moreover, the proposed system has performed better concerning ease of operation, correctness, and efficiency. Further, a comparative analysis has been done with the adaptive controllers employed in the SHAF. The comparison has been performed between ANF-LMS and ANF-RLS techniques with the DCC method under balanced and unbalanced load. From the test results, it was observed that the efficiency of harmonic elimination in ANF–RLS has been found suitable as compared to the ANF-LMS technique. The ANF-RLS has been utilized in designing the PV-APF system, which indicates better performances as compared to the other techniques. The simulation outputs have signified that the proposed system can perform simultaneously two works, one by providing maximum power from a PV unit and second by compensating the current harmonics in non-linear loads. Moreover, it was also examined that the reactive power control and THD improvements were much improved in ANF-RLS as compared to that of ANF-LMS.

References

[1] Naqvi SB, Kumar S, Singh B. Three-Phase Four-Wire PV System for Grid Interconnection at Weak Grid Conditions. IEEE Transactions on Industry Applications. 2020 Sep 1;56(6):7077-87.

[2] Das SR, Mishra AK, Ray PK, Mohanty A, Mishra DK, Li L, Hossain MJ, Mallick RK. Advanced wavelet transform based shunt hybrid active filter in PV integrated power distribution system for power quality enhancement. IET Energy Systems Integration. 2020 Dec;2(4):331-43.

[3] Mao M, Cui L, Zhang Q, Guo K, Zhou L, Huang H. Classification and summarization of solar photovoltaic MPPT techniques: A review based on traditional and intelligent control strategies. Energy Reports. 2020 Nov 1;6: 1312-27.

[4] M. Balamurugan, S.K. Sahoo, and S. Sukchai, Application of soft computing methods for grid connected PV system: a technological and status review, Renewable and Sustainable Energy Reviews. 75 (2017) 1493-1508.

[5] LL Jiang, R Srivatsan, DL Maskell. Computational intelligence techniques for maximum power point tracking in PV systems: A review." Renewable and Sustainable Energy Reviews 85 (2018): 14-45.

[6] Das SR, Sahoo AK, Dhiman G, Singh KK, Singh A. Photo voltaic integrated multilevel inverter based hybrid filter using spotted hyena optimizer. Computers & Electrical Engineering. 2021 Dec 1;96:107510.

[7] T Laagoubi, M Bouzi, M Benchagra. MPPT and power factor control for grid connected PV systems with fuzzy logic controllers. International Journal of Power Electronics and Drive Systems 9, no. 1 (2018): 105.

[8] S Assahout, H Elaissaoui, A El Ougli, B. Tidhaf, and H. Zrouri. A neural network and fuzzy logic based MPPT algorithm for photovoltaic pumping system. International Journal of Power Electronics and Drive Systems 9, no. 4 (2018): 1823.

[9] A Harrag, S Messalti. IC-based variable step size neuro-fuzzy MPPT improving PV system performances. Energy Procedia 157 (2019): 362-374.

[10] O Zamzoum, A Derouich, S Motahhir, Y El Mourabit, A El Ghzizal. Performance analysis of a robust adaptive fuzzy logic controller for wind turbine power limitation. Journal of Cleaner Production. 2020 Apr 25:121659.

[11] H Rezk, M Aly, M Al-Dhaifallah, M Shoyama. Design and Hardware Implementation of New Adaptive Fuzzy Logic-Based MPPT Control Method for Photovoltaic Applications, IEEE Access, 7 (2019): 106427-106438.

[12] Das SR, Ray PK, Sahoo AK, Ramasubbareddy S, Babu TS, Kumar NM, Elavarasan RM, Mihet-Popa L. A Comprehensive Survey on Different Control Strategies and Applications of Active Power Filters for Power Quality Improvement. Energies. 2021 Jan;14(15):4589.

[13] R. M. Kamel, New inverter control for balancing standalone micro-grid phase voltages: A review on MG power quality improvement, Renewable and Sustainable Energy Reviews, 63 (2016) 520-532.

[14] M. Badoni, A. Singh, B. Singh, Comparative performance of wiener filter and adaptive least mean square-based control for power quality improvement. IEEE Transactions on Industrial Electronics. 63(5) (2016) 3028-3037.

[15] S. Agrawal, D. K Palwalia, M. Kumar. "Performance analysis of ann based three-phase four-wire shunt active power filter for harmonic mitigation under distorted supply voltage conditions." IETE Journal of Research (2019): 1-9.

[16] Lam, Chi-Seng, Lei Wang, Sut-Ian Ho, and Man-Chung Wong. "Adaptive thyristor-controlled LC-hybrid active power filters for reactive power and current harmonics

compensation with switching loss reduction." IEEE Transactions on Power Electronics 32, no. 10 (2016): 7577-7590.

[17] Karthikeyan, M., K. Sharmilee, P. M. Balasubramaniam, N. B. Prakash, M. Rajesh Babu, V. Subramaniyaswamy, and S. Sudhakar. "Design and implementation of ANN-based SAPF approach for current harmonics mitigation in industrial power systems." Microprocessors and Microsystems 77 (2020): 103194.

[18] Golestan, S., Guerrero, J.M., Gharehpetian, G.: Five approaches to deal with problem of DC offset in phase-locked loop algorithms: design considerations and performance evaluations. IEEE Trans Power Electron 31(1), 648–660 (2016).

[19] Ibarra, L., Ponce, P., Ayyanar, R. and Molina, A., 2020. A non-adaptive single-phase PLL based on discrete half-band filtering to suppress severe frequency disturbances. Energies, 13(7), p.1730.

[20] A. Rohani, M. Joorabian, M. Abasi, and M. Zand. Three-phase amplitude adaptive notch filter control design of DSTATCOM under unbalanced/distorted utility voltage conditions. Journal of Intelligent & Fuzzy Systems 37, no. 1 (2019): 847-865.

[21] Li, Jinbo, Qin Wang, Lan Xiao, Zehao Liu, and Qunfang Wu. "An accurate and robust adaptive notch filter-based phase-locked loop." Journal of Power Electronics 20, no. 6 (2020): 1514-1525.

[22] Khazraj, Hesam, F. Faria da Silva, Claus Leth Bak, and Saeed Golestan. "Analysis and design of notch filter-based PLLs for grid-connected applications." Electric Power Systems Research 147 (2017): 62-69.

[23] Singh S, Kewat S, Singh B, Panigrahi BK. Enhanced momentum LMS-based control technique for grid-tied solar system. IET Power Electronics. 2020 Oct 15;13(13):2767-74.

[24] Radek Martinek, Jan Zidek, Petr Bilik, Jakub Manas, Jiri Koziorek, Zhaosheng Teng, He Wen, et al. The use of LMS and RLS adaptive algorithms for an adaptive control method of active power filter. Energy and Power Engineering, 5(04):1126, 2013.

[25] Gupta A. Influence of solar photovoltaic array on operation of grid-interactive fifteen-level modular multilevel converter with emphasis on power quality. Renewable and Sustainable Energy Reviews. 2017 Sep 1;76:1053-65.